Differential mobilization of terrestrial carbon pools in Eurasian Arctic river basins

Xiaojuan Feng[a,b,1], Jorien E. Vonk[a,c], Bart E. van Dongen[d], Örjan Gustafsson[e], Igor P. Semiletov[f,g], Oleg V. Dudarev[g], Zhiheng Wang[h], Daniel B. Montluçon[a,b], Lukas Wacker[i], and Timothy I. Eglinton[a,b]

[a]Geological Institute, Eidgenössiche Technische Hochschule Zürich, 8092 Zurich, Switzerland; [b]Department of Marine Chemistry and Geochemistry, Woods Hole Oceanographic Institution, Woods Hole, MA 02543; [c]Department of Earth Sciences, Utrecht University, 3584 CD Utrecht, The Netherlands; [d]School of Earth, Atmospheric, and Environmental Sciences and the Williamson Research Centre for Molecular Environmental Science, University of Manchester, Manchester M13 9PL, United Kingdom; [e]Department of Applied Environmental Science and the Bolin Centre for Climate Research, Stockholm University, 10691 Stockholm, Sweden; [f]International Arctic Research Center, University of Alaska, Fairbanks, AK 99775-7340; [g]Pacific Oceanological Institute, Russian Academy of Sciences, Far Eastern Branch, Vladivostok 6900, Russia; [h]Center for Macroecology, Evolution, and Climate, Department of Biology, University of Copenhagen, DK-2100 Copenhagen, Denmark; and [i]Laboratory of Ion Beam Physics, Eidgenössiche Technische Hochschule Zürich, 8093 Zurich, Switzerland

Edited* by John M. Hayes, Woods Hole Oceanographic Institution, Woods Hole, MA, and approved July 23, 2013 (received for review April 13, 2013)

Mobilization of Arctic permafrost carbon is expected to increase with warming-induced thawing. However, this effect is challenging to assess due to the diverse processes controlling the release of various organic carbon (OC) pools from heterogeneous Arctic landscapes. Here, by radiocarbon dating various terrestrial OC components in fluvially and coastally integrated estuarine sediments, we present a unique framework for deconvoluting the contrasting mobilization mechanisms of surface vs. deep (permafrost) carbon pools across the climosequence of the Eurasian Arctic. Vascular plant-derived lignin phenol ^{14}C contents reveal significant inputs of young carbon from surface sources whose delivery is dominantly controlled by river runoff. In contrast, plant wax lipids predominantly trace ancient (permafrost) OC that is preferentially mobilized from discontinuous permafrost regions, where hydrological conduits penetrate deeper into soils and thermokarst erosion occurs more frequently. Because river runoff has significantly increased across the Eurasian Arctic in recent decades, we estimate from an isotopic mixing model that, in tandem with an increased transfer of young surface carbon, the proportion of mobilized terrestrial OC accounted for by ancient carbon has increased by 3–6% between 1985 and 2004. These findings suggest that although partly masked by surface carbon export, climate change-induced mobilization of old permafrost carbon is well underway in the Arctic.

fluvial mobilization | compound-specific ^{14}C | hydrogeographic control

Arctic permafrost, storing approximately half of the global reservoir of soil organic carbon (OC) (1), is suggested to be highly sensitive to warming-induced perturbation and mobilization (2). Although increased respiration of permafrost carbon has recently been documented with warming (3) and thawing (4) in Arctic soils, information on the large-scale mobilization of old carbon deposits via fluvial and coastal processes remains sparse (5, 6). As permafrost thaws, the active layer deepens and landscape structures collapse and erode, potentially releasing OC of older ages from deeper horizons into rivers and/or coastal oceans (2, 5, 7). Alteration in permafrost coverage also affects the availability of various hydrological conduits, and thus mobilization pathways of OC associated with different permafrost depths and structures (6, 8). As important processes of carbon dispersal in the Arctic, fluvial transport and erosion are hence sensitive to climatic and hydrological changes (8–12). Furthermore, Arctic rivers provide an integrating perspective on carbon release from various OC pools associated with heterogeneous physiogeographic regimes in corresponding drainage basins (13). The central challenge to detecting climate-induced mobilization of permafrost is to distinguish the aged permafrost carbon among the diverse OC components carried in rivers (ranging from modern vegetation debris and plankton to ancient sedimentary rock) (5, 14, 15) and to separate the effect of warming from other hydrogeographic controls on carbon export from different pools.

Source-tracing organic molecules offer a unique perspective into the fate of specific carbon pools during fluvial and coastal transport (6, 16–19). As the second most abundant biopolymer and rigidifying tissue in terrestrial vascular plants, lignin represents both an excellent tracer and a quantitatively significant fraction of terrestrial OC (20). The radiocarbon age of lignin-derived phenols in sediments potentially provides an additional dimension of information on the source (recent surface OC vs. old permafrost OC) and mobilization pathways of higher plant-derived carbon in the Arctic. Furthermore, Arctic soils contain significant carbon inputs from moss-dominated peat (21, 22), which represents 17% of permafrost carbon in the Northern Hemisphere (1). Although this carbon pool does not contain lignin, it can be traced by hydroxy phenols (including *p*-hydroxybenzaldehyde, *p*-hydroxyacetophenone, and *p*-hydroxybenzoic acid) that occur in higher abundances in mosses and peat than in vascular plants (23–25). Here, we examine the radiocarbon signature of lignin-derived and hydroxy phenols in estuarine surface sediments across the Eurasian Arctic to compare the fate of various terrestrial OC pools transported over continental drainage basin scales and to exploit their ^{14}C signals as tracers for permafrost carbon mobilization.

Using estuarine sediments as natural integrators of coastal and drainage basin processes, this study includes the estuaries of five great Russian Arctic rivers (GRARs: Ob, Yenisey, Lena, Indigirk, and Kolyma), extended westward by the Kalix River draining Scandinavia north of the Arctic Circle (Fig. 1). The transect covers a continent-scale climate gradient from west to east (Fig. 2*A* and Table S1). The three eastern GRARs (Lena, Indigirka, and Kolyma) are predominantly located in the continuous permafrost region with a drier and colder climate (26). This contrasts with the two western GRARs (Ob and Yenisey) and the Kalix River, which drain a wetter region rich in peatland and wetlands underlain by discontinuous permafrost (27, 28). These contrasting drainage basin characteristics allow us to investigate the hydroclimatic processes controlling the release and transport of Arctic carbon pools.

Author contributions: X.F., Ö.G., and T.I.E. designed research; X.F., J.E.V., B.E.v.D., Ö.G., I.P.S., O.V.D., and D.B.M. performed research; X.F., D.B.M., L.W., and T.I.E. contributed new reagents/analytic tools; X.F. and Z.W. analyzed data; and X.F., J.E.V., Ö.G., and T.I.E. wrote the paper.

The authors declare no conflict of interest.

*This Direct Submission article had a prearranged editor.

[1]To whom correspondence should be addressed. E-mail: xfeng@erdw.ethz.ch.

This article contains supporting information online at www.pnas.org/lookup/suppl/doi:10.1073/pnas.1307031110/-/DCSupplemental.

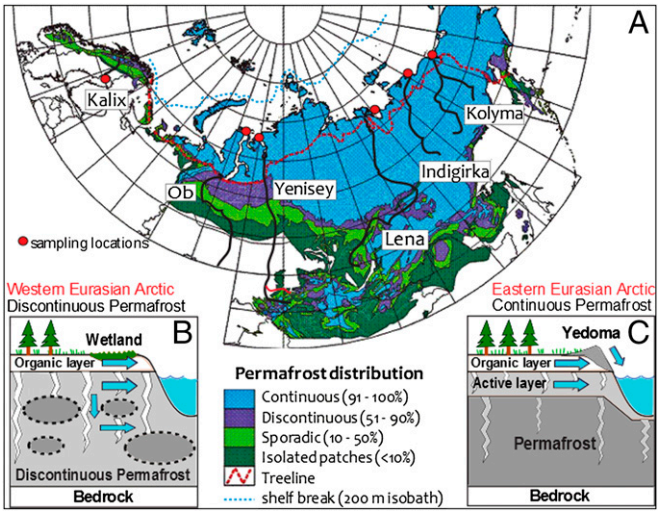

Fig. 1. Eurasian Arctic transect and cartoon of hydrological mobilization of terrestrial carbon into rivers. (*A*) Map of the rivers (black lines) with permafrost distribution (modified from refs. 1 and 6) and sampling locations (red circles). (*B*) Illustration of the western Eurasian Arctic characterized by extensive moss-dominated wetlands underlain by discontinuous permafrost and ubiquitous deep groundwater conduits. (*C*) Illustration of eastern Eurasian Arctic characterized by a wide distribution of Yedoma ice complex, a thin seasonally thawing active layer, and thick continuous permafrost below. Blue arrows indicate hydrological transport of carbon from different physiogeographic regimes.

Results and Discussion

Contrasting ^{14}C Characteristics of Terrestrial OC Components. We used a recently modified method (29) to isolate lignin and hydroxy phenols from sedimentary matrices for compound-specific radiocarbon analysis. The radiocarbon content of OC components from estuarine surface sediments affords an average age of terrestrial OC released from the adjacent fluvial drainage basin and via coastal erosion processes. Individual lignin phenols exhibited relatively uniform Δ^{14}C values (−402 to −367‰) in the Indigirka and Kolyma sediments, whereas much higher isotopic variability was observed in sediments from the Kalix and Ob (Fig. S1*A*), implying greater heterogeneity in lignin sources and/or more complex mobilization pathways in the western Eurasian Arctic watersheds. Nevertheless, there was no significant age offset between vanillyl and syringyl phenols in the same estuarine sediments (*t* test, $P > 0.05$; Fig. S1*B*). Concentration-weighted average Δ^{14}C values of lignin phenols ranged from −385 to +33‰ across the Eurasian Arctic transect, corresponding to conventional radiocarbon ages of 3,800 y to modern (Fig. 2*B*). It is notable that lignin phenols largely follow the trend of bulk OC radiocarbon ages (ranging from 570 to 7,500 y; Fig. 2*B*), reflecting the role of lignin as a tracer of a major fraction of terrestrial OC during land–ocean transfer. The age offset between lignin phenols and bulk OC was substantially higher in the three eastern GRARs (2,000–4,000 ^{14}C y) than in the three western rivers (<700 y; Fig. 2*B*), however. Because these estuarine sediments have all been shown to be dominated by terrestrial OC with very minor contributions from rock-derived fossil carbon (26, 30), the larger age offsets in eastern GRARs likely reflect the larger contribution of old OC from erosion of the loess-like Yedoma ice complex that is prevalent in East Siberia (5, 13, 31).

Interestingly, the ^{14}C ages of lignin phenols were substantially younger than those of another suite of terrestrial OC tracer compounds, long-chain higher plant leaf wax lipids (32) [$C_{27,29,31}$ *n*-alkanes and $C_{24,26,28}$ *n*-alkanoic acids ranging from 5,500 to 13,600 ^{14}C y in age (6)], previously measured in these sediment samples (Fig. 2*B*). The Δ^{14}C offset between lignin phenols and plant wax lipids increased from ∼160–180‰ in the continuous permafrost region (Kolyma and Indigirka) to ∼700‰ in the western watershed (Kalix), which has much lower permafrost coverage (Fig. 2*A*), corresponding to a ^{14}C age offset of up to 13,000 y (Fig. 2*B*). The sharply contrasting ^{14}C characteristics suggest varied carbon sources and/or transfer mechanisms for these two groups of higher plant markers. In contrast to lignin, which is enriched in woody debris and coarse soil particles (33, 34), plant wax lipids are closely associated with fine-grained minerals and preferentially stabilized in deep mineral soils (34). Therefore, although plant wax lipids constitute a smaller component of the terrestrial OC (Table S2), their old ^{14}C ages reveal the mobilization of a preaged (deep permafrost soil) carbon pool. By comparison, lignin phenols appear to trace relatively recent OC inputs supplied from surface layers (organic and surface soil horizons).

Hydroxy phenols displayed another distinct pattern in their Δ^{14}C values across the transect, with similar values to lignin phenols observed in two western rivers (−383‰ and +22‰ in the Ob and Kalix, respectively) and values lower than lignin phenols but comparable to plant wax lipids in the three eastern GRARs (−529 to −477‰; Fig. 2*B* and Fig. S1*B*). Because wetlands dominated by *Sphagnum* mosses constitute a high proportion of the Ob and Kalix basins (27, 28) (Table S1), hydroxy phenols predominantly record OC inputs from contemporary wetlands in these watersheds, and hence bear a similar age to the surface OC pool (represented by lignin phenols). In contrast, East Siberia has a very low wetland coverage (Fig. 2*A* and Table S1) but stores ancient peat deposits enriched in hydroxy phenols in permafrost soils (2, 13). Such old carbon may be released through cryoturbation, thermokarst, and/or bank erosion processes (5, 35), contributing to the older ages of hydroxy phenols relative to lignin phenols in eastern GRARs. These observations suggest that hydroxy phenols incorporate

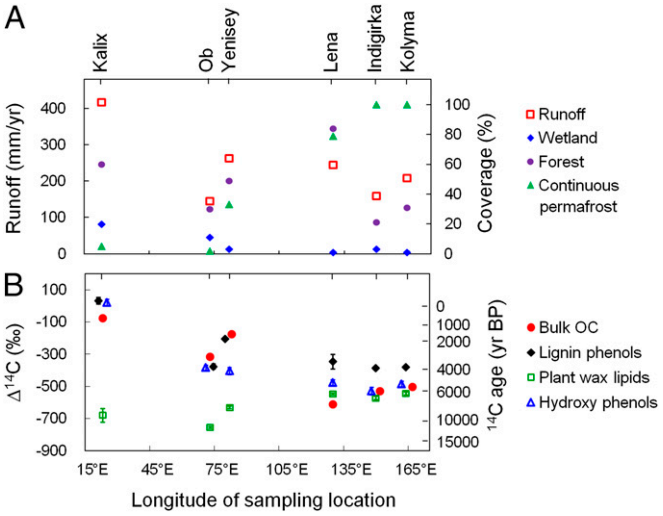

Fig. 2. Hydrogeographic characteristics of the Eurasian Arctic rivers (*A*) and contrasting radiocarbon contents (expressed as Δ^{14}C and conventional ^{14}C age) of terrestrial markers compared with bulk OC in the estuarine surface sediments (*B*). Runoff rate = discharge/basin area. Detailed hydrogeographic data are listed in Table S1 [compiled from refs. 6, 9, 27, 52 and "watersheds of the world" (http://www.wri.org/publications)]. The Δ^{14}C values of terrestrial markers represent concentration-weighted averages with the SEs of analytical measurement propagated. Lignin phenols refer to vanillyl and syringyl phenols (detailed data are provided in Fig. S1). Hydroxy phenols refer to *p*-hydroxybenzaldehyde, *p*-hydroxyacetophenone, and *p*-hydroxybenzoic acid. Plant wax lipids constitute *n*-alkanes ($C_{27,29,31}$) and *n*-alkanoic acids ($C_{24,26,28}$) (6).

carbon released from both surface and deep OC pools across the transect.

Hydrogeographic Controls on the Mobilization of Different OC Pools. In accordance with the above interpretations, mobilization of each carbon pool is mediated by different physiogeographic and hydrological variables across the drainage basins (Fig. 2*A*, Fig. S2, and Table S1). Among the investigated physiogeographic variables, runoff exerts a strong control on the $\Delta^{14}C$ values of lignin phenols across the Eurasian Arctic ($P < 0.01$, $R^2 = 0.92$; Fig. 3*A*), where younger lignin is transported by rivers with a higher mean annual runoff rate. This correlation is consistent with the efficient delivery of vascular plant debris during storm, flood, and high-precipitation events (36–38), suggesting increased transfer of surface detrital carbon in high-runoff systems. It is notable that at zero runoff rate (representing extreme base flow with minimum detrital input), regression analysis yields an end-member $\Delta^{14}C$ value of −655‰ for lignin phenols, similar to that of plant wax lipids in the westernmost (Kalix) estuary. Assuming that surface detrital carbon has decadal turnover times in the high latitudes (39, 40), and hence a $\Delta^{14}C$ value of +100 to +200‰, whereas deep soil-derived lignin has a $\Delta^{14}C$ value of −655‰, we estimate from a binary mixing model (Table S3) that ∼30–90% of mobilized lignin across the Eurasian Arctic reflects modern carbon sources.

In contrast, the $\Delta^{14}C$ values of plant wax lipids are most strongly correlated with the watershed coverage of continuous permafrost ($P < 0.01$, $R^2 = 0.86$; Fig. 3*B*) but not with runoff ($P = 0.85$; Fig. S2), consistent with enhanced mobilization of deep, old permafrost carbon in discontinuous permafrost systems. This phenomenon may be associated with multiple processes. As continuous permafrost shifts to more discontinuous or sporadic permafrost regimes westward in the transect, more hydraulic conduits are accessible in the deep soil (Fig. 1 *B* and *C*), leading to the release of older carbon pools that are enriched in lipids relative to lignin. Moreover, thermokarst and thermal erosion processes potentially increase from perennially frozen regions to warmer, seasonally frozen zones (12, 41), enabling faster mobilization of deep OC from river banks and coastlines. Although erosion may also play a part in releasing lignin-rich OC from surface layers, its effect seems to be dwarfed by surface runoff processes because neither temperature nor permafrost coverage is correlated with the lignin age (Fig. S2). Hence, transport of younger lignin is enhanced in the river with the highest runoff rate (Kalix; Fig. 2*A*), leading to a larger age offset between lignin phenols and plant wax lipids toward the west end of the transect (Fig. 2*B*).

By comparison, corresponding $\Delta^{14}C$ values for hydroxy phenols were best correlated with the wetland coverage in the drainage basin ($P < 0.01$, $R^2 = 0.86$; Fig. 3*C*) and, to a lesser degree, with the mean annual runoff rate ($P = 0.03$, $R^2 = 0.74$; Fig. 3*D*). This suggests that contemporary wetlands are the main source of modern hydroxy phenols across the Eurasian Arctic, whose delivery from surface litter and soil layers is, similar to lignin phenols, influenced by runoff processes. Moreover, in the $\Delta^{14}C$-runoff correlation plot (Fig. 3*D*), the hydroxy-phenol $\Delta^{14}C$ values of four eastern rivers all fall below the general trend line (black line) and have a much flatter slope against the runoff rate (blue line; $P < 0.05$, $R^2 = 0.81$). This suggests that surface runoff is less efficient in supplying modern hydroxy phenols in the watersheds with a low wetland coverage, where inputs of old hydroxy phenols from deeper soils are prominent.

Contribution of Surface and Deep Permafrost Carbon to Bulk Sedimentary OC. Our molecular radiocarbon data show that detrital carbon from recent vegetation and surface organic layers is a key component of the mobilized terrestrial carbon in the Eurasian Arctic that accumulates in estuarine sediments. To evaluate

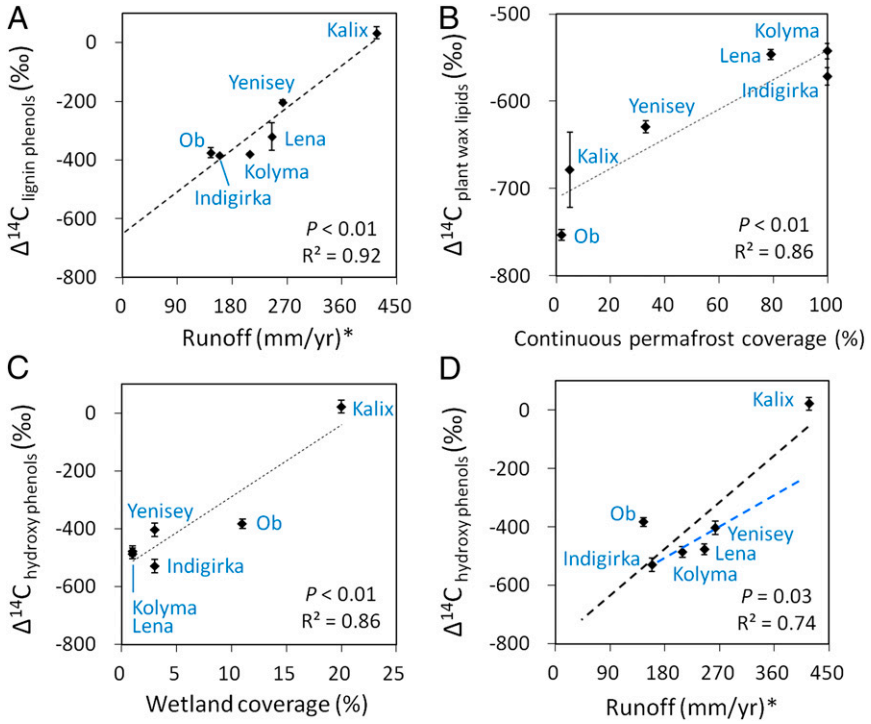

Fig. 3. Hydrological and physiogeographic controls on the age of terrestrial markers in the integrating Eurasian Arctic estuaries: correlation of $\Delta^{14}C_{\text{lignin phenols}}$ with runoff rate (*A*), $\Delta^{14}C_{\text{plant wax lipids}}$ with continuous permafrost coverage (*B*), $\Delta^{14}C_{\text{hydroxy phenols}}$ with wetland coverage (*C*), and $\Delta^{14}C_{\text{hydroxy phenols}}$ with runoff rate (*D*). The blue dotted line in *D* represents linear correlation for the data of four eastern rivers ($P < 0.05$, $R^2 = 0.81$). *Runoff rate = discharge/basin area. Contents of terrestrial markers are defined in Fig. 2. Further statistical analyses can be found in Fig. S2.

the magnitude of permafrost carbon release, we first need to assess the contribution of surface and deep permafrost carbon pools to the bulk OC. Clearly, this is complicated due to inputs from other organic components [e.g., black carbon (42, 43) and planktonic carbon (5)], as underlined by the age difference of bulk OC relative to the terrestrial markers in the Lena, Ob, and Yenisey sediments (Fig. 2*B*). Assuming that hydroxy phenols incorporate the isotopic signal of terrestrial biospheric carbon derived from both surface and deep carbon sources, whereas the $\Delta^{14}C$ values of lignin phenols and plant wax lipids represent the integrated radiocarbon signal of mobilized surface and deeper permafrost OC pools in each watershed, respectively, we estimate from a binary mixing model that 47–77% of terrestrial biospheric carbon originates from deeper permafrost in the four eastern river basins (where the modern wetland carbon contribution is small; Table S4). This estimate likely represents a lower limit, because the surface OC end member (lignin) also incorporates a significant amount of preaged OC from surface soil horizons. Nonetheless, it implies that over half of the sedimentary OC in East Siberian estuaries originates from a previously stabilized or ancient soil pool, consistent with a recent estimate that 36–76% of sedimentary OC in the East Siberian Arctic Shelf is derived from erosion of Pleistocene Yedoma (5).

During the second half of the 20th century, Eurasian Arctic river runoff increased at an average rate of ∼0.60–0.74 mm/y (44–46), likely increasing the delivery of surface-derived OC into estuaries. Based on the relationship between lignin phenol $\Delta^{14}C$ values and runoff ($\Delta^{14}C = 1.6018 \times \text{runoff} - 655$; Fig. 3*A*), the $\Delta^{14}C$ value of mobilized surface OC has increased by ∼19–24‰ from 1985 to 2004, not considering the variation of bomb-derived ^{14}C in the atmosphere. This time window corresponds to the sediment-deposition time of 20 y, based on the surface sediment depth and sedimentation rate in the region (5). Assuming that the ^{14}C signals of exported OC have remained similar during this period and that the end-member $\Delta^{14}C$ value of deep permafrost OC has not altered, we estimate that the proportion of ancient OC in the total terrestrial carbon pool has increased by 3–6% in four eastern GRAR sediments (Table S4) over this period. When we assume that particulate organic carbon (POC) fluxes in these rivers (Table S1) are dominantly terrestrial in origin (26, 30), the 20-y increase is equivalent to ∼1.4 teragrams of carbon transferred from old permafrost into estuarine sediments. Although this number represents a rough estimate and is relatively small compared with some other Arctic carbon fluxes (47), release of dissolved OC (23, 47, 48) and water-column mineralization of POC (5, 49) associated with permafrost thawing may well exceed the size of this sediment OC budget in the context of a changing climate. Our estimate represents a conservative scenario because sedimentary $\Delta^{14}C$ values are postulated to decrease further with warming. Furthermore, particle transit time, albeit not well constrained, is likely to be longer than a few decades in these rivers, given the residence time of suspended sediments in large meandering rivers [∼17,000 y in the Amazon River (50)] and woody debris in small mountainous rivers [∼20 y (51)]. The young terrestrial OC components mobilized into these sediments from 1985 to 2004 were hence likely derived from materials deposited in the surface layers before the 1980s and had an even larger increase in $\Delta^{14}C$ values due to the incorporation of bomb-derived ^{14}C into surface decadal OC pools (40). These calculations suggest that the magnitude of permafrost carbon release, which may be masked or muted by other Arctic OC pools, is relevant on regional to continental scales.

Implications for Arctic Carbon Cycling. Our results reveal marked age offsets between different terrestrial OC pools released from Arctic landscapes, which stands in contrast to some temperate and tropical systems, where terrestrial OC components are retained on land for a similar period [e.g., the Columbia River (29)]. These findings highlight the linkage between carbon cycling and hydrological processes, which is particularly close in Arctic landscapes, where surface and groundwater flows access different pools of carbon depending on the spatial distribution of permafrost. Surface runoff appears to control the release of a major component of terrestrial carbon, whereas deep hydraulic conduits and bank/coastal erosion may mobilize very old permafrost carbon at depth. This observation reveals an important caveat in deriving OC budgets or reconstructing past carbon dynamics in the Arctic system based on bulk sedimentary OC properties, because end-member values may vary substantially due to the release of significantly preaged soil carbon. Molecular-level ^{14}C measurements enable constraints to be placed on the relative contribution of surface and deep permafrost carbon pools to Arctic fluvial export. Unraveling such hydrogeographic controls on the differential delivery of Arctic carbon pools is key to unmasking warming effects on permafrost carbon release. As such, our data suggest that export of old deep permafrost OC as a consequence of recent climate variations may be underestimated and masked by the synoptic increase in the transport of young surface OC associated with enhanced river runoff in the Arctic. The ability to differentiate and separately trace mobilized carbon pools across the Arctic will aid in refining both our understanding of the contemporary system and our ability to predict linkages between a warming climate and the mobilization of Arctic permafrost carbon.

Materials and Methods

Study Area. The three eastern GRARs (Lena, Indigirka, and Kolyma) drain into the Laptev Sea (Lena) and the East Siberian Sea (Indigirka and Kolyma) (Fig. 1*A*). The climate in the drainage basin is semiarid to arid, with average summer temperatures between +7 °C and +9 °C and winter temperatures below −40 °C. This contrasts with the two western GRARs (Ob and Yenisey) located in the western Siberian lowland and the Kalix River, which drains from sub-Arctic Scandinavia into the Baltic Sea. The drainage basins have average summer temperatures comparable to northeastern Eurasia but much higher winter temperatures (around −20 °C) (28) and are wetter, with higher precipitation-to-evaporation ratios compared with eastern GRARs. All rivers have comparable drainage area-normalized fluxes of total organic carbon (TOC) and POC (27, 52) (Table S1). A more detailed description of the river drainage basins is provided elsewhere (26, 30). Surface sediments (0–2 cm) were collected using a grab sampler from the GRAR estuaries during the second and third Russia–United States cruises (on *HIV Ivan Kireev*) in 2004 and 2005 and from the Kalix in 2005 on the research vessel *KBV005* from the Umeå Marine Research Center (Norrbyn, Sweden). These sediments were mainly delivered by the annual spring freshet of the rivers and by coastal erosion during the past ∼20 y based on the sedimentation rate of 0.11–0.16 cm/y (5, 26). Previous molecular and isotopic investigations revealed a predominance of terrestrial OC with very minor contributions from aquatic biomass or petrogenic (rock-derived) carbon into these estuarine sediments (26, 30).

Bulk Analyses. Bulk sediments were kept frozen at −20 °C after collection and were freeze-dried before analysis. A small aliquot was used for TOC and bulk $\delta^{13}C$ analyses at the University of California, Davis Stable Isotope Facility (http://stableisotopefacility.ucdavis.edu) and for bulk $\Delta^{14}C$ analysis at the National Ocean Sciences Accelerator Mass Spectrometry (NOSAMS) Facility at Woods Hole Oceanographic Institution.

Isolation and ^{14}C Analysis of Individual Compounds. As described previously (6), lipids were extracted from freeze-dried sediments (∼30–70 g) using Soxhlet extraction with dichloromethane/methanol (2:1, 24 h). Plant wax *n*-alkanes and *n*-alkanoic acids were isolated using preparative capillary GC and analyzed for ^{14}C content. The solvent-extracted residues were further hydrolyzed with 1 M KOH in methanol (100 °C, 3 h) to remove hydrolysable lipids. The dried residues were then subjected to alkaline CuO oxidation to release lignin and hydroxy phenols on a microwave system (MARS; CEM Corporation) (53). For each sample, ∼5 g of CuO, 0.6 g of ferrous ammonium sulfate, and 25 mL of N_2-bubbled NaOH solution (2 M) were loaded into each of five to eight vessels containing sediments (3–10 g) with ∼50 mg of TOC. Vessels containing all reagents but no sample were also included as procedural blanks along with each batch of sediments.

For compound-specific radiocarbon analysis, phenolic compounds were isolated using an HPLC-based method [*SI Materials and Methods*; details are provided by Feng et al. (29)]. Briefly, the CuO oxidation extracts were purified through two solid-phase extraction (SPE) cartridges (Supelco Supelclean ENVI-18 and Supelclean LC-NH_2 SPEs) and separated through two HPLC isolation steps consisting of a Phenomenex Synergi Polar-RP column and a ZORBAX Eclipse XDB-C18 column. Approximately 10–150 μg of carbon of individual phenols was collected using a fraction collector, yielding purities >99%. Procedural blanks were processed in the same manner for subsequent blank corrections.

Purified phenols were combusted under vacuum at 850 °C for 5 h. The resulting CO_2 was cryogenically purified and quantified. A batch of CO_2 samples (~23–150 μg of carbon) was sent to NOSAMS, graphitized, and measured on accelerator mass spectrometry (AMS). A second batch of CO_2 samples (~10–32 μg carbon) was directly measured without graphitization on the miniaturized radiocarbon dating system at the Eidgenössiche Technische Hochschule Zürich using a gas feeding system (54). Radiocarbon contents are reported as $\Delta^{14}C$ (‰) and conventional ^{14}C age. Procedural blanks associated with the extraction/HPLC/combustion procedures yielded 2.5 ± 0.8 μg of carbon with a fraction modern (Fm) value of 0.21 ± 0.07 (n = 5). All radiocarbon values are corrected for procedural blanks with the errors propagated. We did not observe a significant difference between radiocarbon contents of the same sample measured at the two AMS facilities.

Binary Mixing Model. We used a ^{14}C binary mixing model to assess the relative contributions of surface OC (Table S3) and permafrost OC (Table S4) to lignin or hydroxy phenol, respectively. The model is expressed in the following two equations:

$$f_S(\Delta^{14}C_S) + f_P(\Delta^{14}C_P) = \Delta^{14}C_{phenol}, \quad [1]$$

$$f_S + f_P = 1, \quad [2]$$

where f is the percentage of surface or permafrost OC and the subscripts S and P refer to surface and permafrost, respectively.

Modeling and Statistical Analysis. A t test was used to compare the ^{14}C content of different phenols. Differences are considered to be significant at a level of $P < 0.05$. Linear regression analysis was used to assess the correlation between drainage basin characteristics and the ^{14}C content of terrestrial OC markers (Fig. S2). The main drainage basin parameters investigated as explanatory variables include basin area; runoff rate; mean annual summer cumulative temperature (ASCT); and the coverage of forest, wetland, and continuous permafrost in the watershed (Table S1). The ASCT is calculated as the sum of mean monthly temperature for months with a mean temperature above 0 °C within a year (details are provided in *SI Materials and Methods* and Fig. S3) and is considered to have a major impact on permafrost thawing (55). POC flux and discharge are found to be correlated with continuous permafrost coverage ($P < 0.05$, $R^2 = 0.85$) and basin area ($P < 0.05$, $R^2 = 0.84$), respectively, and are hence not included as basin parameters in the ^{14}C correlation analyses. Correlation is considered to be significant at a level of $P < 0.05$, and the R^2 values are used to compare the explanatory power of the variables.

ACKNOWLEDGMENTS. We thank all colleagues in the International Siberian Shelf Study (ISSS) Program for support, including sampling. We thank Li Xu for assistance with AMS analyses at Woods Hole Oceanographic Institution (WHOI). Christopher Reddy is acknowledged for providing access to an HPLC system. Grants OCE-9907129, OCE-0137005, and OCE-0526268 from the US National Science Foundation, the Stanley Watson Chair for Excellence in Oceanography (to T.I.E.), and Eidgenössiche Technische Hochschule (ETH) Zürich enabled this research. Ö.G. acknowledges an Academy Research Fellow grant from the Swedish Royal Academy of Sciences. J.E.V. thanks the Netherlands Organization for Scientific Research-Rubicon (Grant 825.10.022) for support. B.E.v.D thanks the UK Natural Environment Research Council (Grant NE/I024798/1) for support. X.F. thanks the WHOI for a postdoctoral scholar fellowship and ETH Zürich for postdoctoral support. The ISSS program is supported by the Knut and Alice Wallenberg Foundation, the Far Eastern Branch of the Russian Academy of Sciences, the Swedish Research Council, the US National Oceanic and Atmospheric Administration, the Russian Foundation of Basic Research, the Swedish Polar Research Secretariat, and the Nordic Council of Ministers (Arctic Cooperation and Top-Level Research Initiative-Defrost programs).

1. Tarnocai C, et al. (2009) Soil organic carbon pools in the northern circumpolar permafrost region. *Global Biogeochem Cycles* 23:GB2023, 10.1029/2008GB003327.
2. Schuur EAG, et al. (2008) Vulnerability of permafrost carbon to climate change: Implications for the global carbon cycle. *Bioscience* 58(8):701–714.
3. Dorrepaal E, et al. (2009) Carbon respiration from subsurface peat accelerated by climate warming in the subarctic. *Nature* 460(7255):616–619.
4. Schuur EAG, et al. (2009) The effect of permafrost thaw on old carbon release and net carbon exchange from tundra. *Nature* 459(7246):556–559.
5. Vonk JE, et al. (2012) Activation of old carbon by erosion of coastal and subsea permafrost in Arctic Siberia. *Nature* 489(7414):137–140.
6. Gustafsson Ö, van Dongen BE, Vonk JE, Dudarev OV, Semiletov IP (2011) Widespread release of old carbon across the Siberian Arctic echoed by its large rivers. *Biogeosciences* 8:1737–1743.
7. Schaefer K, Zhang T, Bruhwiler L, Barrett AP (2011) Amount and timing of permafrost carbon release in response to climate warming. *Tellus* 63B(2):165–180.
8. Guo L, Ping CL, Macdonald RW (2007) Mobilization pathways of organic carbon from permafrost to Arctic rivers in a changing climate. *Geophys Res Lett* 34:L13603, 10.11029/12007GL030689.
9. Holmes RM, et al. (2013) *Climatic Change and Global Warming of Inland Waters: Impacts and Mitigation for Ecosystems and Societies*, eds Goldman CR, Kumagai M, Robarts RD (Wiley, Chichester, UK), pp 3–26.
10. Charkin AN, et al. (2011) Seasonal and interannual variability of sedimentation and organic matter distribution in the Buor-Khaya Gulf: The primary recipient of input from Lena River and coastal erosion in the southeast Laptev Sea. *Biogeosciences* 8:2581–2594.
11. Semiletov IP, Shakhova NE, Sergienko VI, Pipko II, Dudarev OV (2012) On carbon transport and fate in the East Siberian Arctic land-shelf-atmosphere system. *Environ Res Lett* 7:015201, 10.1088/1748-9326/7/1/015201.
12. Costard F, et al. (2007) Impact of the global warming on the fluvial thermal erosion over the Lena River in central Siberia. *Geophys Res Lett* 34:L14501, 10.1029/2007GL030212.
13. Schirrmeister L, et al. (2011) Fossil organic matter characteristics in permafrost deposits of the northeast Siberian Arctic. *J Geophys Res* 116:G00M02, 10.1029/2011JG001647.
14. Raymond PA, Bauer JE (2001) Riverine export of aged terrestrial organic matter to the North Atlantic Ocean. *Nature* 409(6819):497–500.
15. Guo L, Macdonald RW (2006) Source and transport of terrigenous organic matter in the upper Yukon River: Evidence from isotope ($\delta^{13}C$, $\Delta^{14}C$, and $\delta^{15}N$) composition of dissolved, colloidal, and particulate phases. *Global Biogeochem Cycles* 20:GB2011, 10.1029/2005GB002593.
16. Kusch S, Rethemeyer J, Schefuss E, Mollenhauer G (2010) Controls on the age of vascular plant biomarkers in Black Sea sediments. *Geochim Cosmochim Acta* 74(24):7031–7047.
17. Karlsson ES, et al. (2011) Carbon isotopes and lipid biomarker investigation of sources, transport and degradation of terrestrial organic matter in the Buor-Khaya Bay, SE Laptev Sea. *Biogeosciences* 8:1865–1879.
18. Dickens AF, Baldock J, Kenna TC, Eglinton TI (2011) A depositional history of particulate organic carbon in a floodplain lake from the lower Ob River, Siberia. *Geochim Cosmochim Acta* 75(17):4796–4815.
19. Vonk JE, et al. (2010) Molecular and radiocarbon constraints on sources and degradation of terrestrial organic carbon along the Kolyma paleoriver transect, East Siberian Sea. *Biogeosciences* 7:3153–3166.
20. Hedges JI, Keil RG, Benner R (1997) What happens to terrestrial organic matter in the ocean? *Org Geochem* 27(5/6):195–212.
21. Hugelius G, Kuhry P (2009) Landscape partitioning and environmental gradient analyses of soil organic carbon in a permafrost environment. *Global Biogeochem Cycles* 23:GB3006, 10.102912008GB102003419.
22. Vonk JE, Gustafsson Ö (2009) Calibrating *n*-alkane Sphagnum proxies in sub-Arctic Scandinavia. *Org Geochem* 40(10):1085–1090.
23. Amon RMW, et al. (2012) Dissolved organic matter sources in large Arctic rivers. *Geochim Cosmochim Acta* 94:217–237.
24. Lehto O, Tuhkanen M, Ishiwatari R, Uzaki M (1985) Quantitative gas chromatographic analysis of degradation and oxidation products from a Finnish *Sphagnum* peat. *Suo (Helsinki)* 36:101–106.
25. Zaccone C, Said-Pullicino D, Gigliotti G, Miano TM (2008) Diagenetic trends in the phenolic constituents of *Sphagnum*-dominated peat and its corresponding humic acid fraction. *Org Geochem* 39(7):830–838.
26. van Dongen BE, Semiletov I, Weijers JWH, Gustafsson Ö (2008) Contrasting lipid biomarker composition of terrestrial organic matter exported from across the Eurasian Arctic by the five great Russian Arctic rivers. *Global Biogeochem Cycles* 22:GB1011, 10.1029/2007GB002974.
27. Ingri J, Widerlund A, Land M (2005) Geochemistry of major elements in a pristine boreal river system; hydrological compartments and flow paths. *Aquat Geochem* 11(1):57–88.
28. Kremenetski KV, et al. (2003) Peatlands of the western Siberian lowlands: Current knowledge on zonation, carbon content and Late Quaternary history. *Quat Sci Rev* 22:703–723.
29. Feng X, et al. (2013) ^{14}C and ^{13}C characteristics of higher plant biomarkers in Washington margin surface sediments. *Geochim Cosmochim Acta* 105:14–30.
30. Vonk JE, van Dongen BE, Gustafsson Ö (2008) Lipid biomarker investigation of the origin and diagenetic state of sub-arctic terrestrial organic matter presently exported into the northern Bothnian Bay. *Mar Chem* 112(1–2):1–10.
31. Romanovskii NN (1993) *Fundamentals of the Cryogenesis of the Lithosphere* (Moscow Univ Press, Moscow).
32. Harwood JL, Russell NJ (1984) *Lipids in Plants and Microbes* (Allen & Unwin, London).

33. Wakeham SG, et al. (2009) Partitioning of organic matter in continental margin sediments among density fractions. *Mar Chem* 115(3–4):211–225.
34. Xu C, Guo L, Ping CL, White DM (2009) Chemical and isotopic characterization of size-fractionated organic matter from cryoturbated tundra soils, northern Alaska. *J Geophys Res* 114:G03002, 10.01029/02008JG000846.
35. Semiletov IP, et al. (2011) Carbon transport by the Lena River from its headwaters to the Arctic Ocean, with emphasis on fluvial input of terrestrial particulate organic carbon vs. carbon transport by coastal erosion. *Biogeosciences* 8:2407–2426.
36. Hilton RG, et al. (2008) Tropical-cyclone-driven erosion of the terrestrial biosphere from mountains. *Nat Geosci* 1(11):759–762.
37. Leithold EL, Hope RS (1999) Deposition and modification of a flood layer on the northern California shelf: Lessons from and about the fate of terrestrial particulate organic carbon. *Mar Geol* 154(1–4):183–195.
38. Smith JC, et al. (2013) Runoff-driven export of particulate organic carbon from soil in temperate forested uplands. *Earth Planet Sci Lett* 365:198–208.
39. Bird MI, Chivas AR, Head J (1996) A latitudinal gradient in carbon turnover times in forest soils. *Nature* 381(6578):143–146.
40. Fröberg M, Tipping E, Stendahl J, Clarke N, Bryant C (2011) Mean residence time of O horizon carbon along a climatic gradient in Scandinavia estimated by ^{14}C measurements of archived soils. *Biogeochemistry* 104(1–3):227–236.
41. Toniolo H, Kodial P, Hinzman LD, Yoshikawa K (2009) Spatio-temporal evolution of a thermokarst in Interior Alaska. *Cold Regions Science and Technology* 56:39–49.
42. Elmquist M, Semiletov I, Guo L, Gustafsson Ö (2008) Pan-Arctic patterns in black carbon sources and fluvial discharges deduced from radiocarbon and PAH source apportionment markers in estuarine surface sediments. *Global Biogeochem Cycles* 22: GB2018, 10.1029/2007GB002994.
43. Guo L, et al. (2004) Characterization of Siberian Arctic coastal sediments: Implications for terrestrial organic carbon export. *Global Biogeochem Cycles* 18:GB1036, 10.1029/2003GB002087.
44. McClelland JW, Dery SJ, Peterson BJ, Holmes RM, Wood EF (2006) A pan-arctic evaluation of changes in river discharge during the latter half of the 20th century. *Geophys Res Lett* 33:L06715, 10.1029/2006GL025753.
45. Peterson BJ, et al. (2002) Increasing river discharge to the Arctic Ocean. *Science* 298(5601):2171–2173.
46. Savelieva NI, Semiletov IP, Vasilevskaya LN, Pugach SP (2000) A climate shift in seasonal values of meteorological and hydrological parameters for Northeastern Asia. *Prog Oceanogr* 47(2–4):279–297.
47. Dittmar T, Kattner G (2003) The biogeochemistry of the river and shelf ecosystem of the Arctic Ocean: A review. *Mar Chem* 83(3–4):103–120.
48. Lobbes JM, Fitznar HP, Kattner G (2000) Biogeochemical characteristics of dissolved and particulate organic matter in Russian rivers entering the Arctic Ocean. *Geochim Cosmochim Acta* 64(17):2973–2983.
49. Sánchez-García L, et al. (2011) Inventories and behavior of particulate organic carbon in the Laptev and East Siberian seas. *Global Biogeochem Cycles* 25:GB2007, 10.1029/2010GB003862.
50. Dosseto A, Bourdon B, Gaillardet J, Maurice-Bourgoin L, Allègre CJ (2006) Weathering and transport of sediments in the Bolivian Andes: Time constraints from uranium-series isotopes. *Earth Planet Sci Lett* 248(3-4):759–771.
51. Hyatt TL, Naiman RJ (2001) The residence time of large woody debris in the Queets River, Washington, USA. *Ecol Appl* 11(1):191–202.
52. Stein R, Macdonald RW (2004) *The Organic Carbon Cycle in the Arctic Ocean* (Springer, Berlin).
53. Goñi MA, Montgomery S (2000) Alkaline CuO oxidation with a microwave digestion system: Lignin analyses of geochemical samples. *Anal Chem* 72(14):3116–3121.
54. Wacker L, et al. (2013) A versatile gas interface for routine radiocarbon analysis with a gas ion source. *Nucl Instrum Methods Phys Res B* 294:315–319.
55. Rinke A, et al. (2012) Arctic RCM simulations of temperature and precipitation derived indices relevant to future frozen ground conditions. *Global Planet Change* 80-81:136–148.

Supporting Information

Feng et al. 10.1073/pnas.1307031110

SI Materials and Methods

Isolation of Lignin Phenols for ^{14}C Analysis. Details of the method are provided by Feng et al. (1). Briefly, the CuO oxidation products (in ethyl acetate) were blown carefully to <100 μL under N_2, redissolved in water (pH 2), and loaded onto a Supelco Supelclean ENVI-18 solid-phase extraction (SPE) cartridge (preconditioned with methanol and water). Lignin oxidation products were eluted with acetonitrile from the ENVI-18 SPE cartridge, blown under N_2 to a volume of <0.5 mL, and further separated on a self-packed amino SPE cartridge (0.5 g, preconditioned with methanol, Supelclean LC-NH_2; Supelco) into phenolic aldehyde/ketone (eluting in methanol) and their corresponding acid (eluting with methanol and 12 M HCl, 95:5) fractions. Each fraction was blown carefully to <100 μL under N_2 and redissolved in methanol for separation on an Agilent 1200 HPLC system coupled to a diode array detector and a fraction collector. Individual phenols were collected through two HPLC isolation steps consisting of a Phenomenex Synergi Polar-RP column (4 μm, 4.6 × 250 mm) with a Polar-RP SecurityGuard column (4 μm, 4.0 × 3.0 mm) and a ZORBAX Eclipse XDB-C18 column (5 μm, 4.6 × 150 mm) with a ZORBAX Eclipse C18 guard column (5 μm, 4.6 × 12.5 mm). The column temperature was maintained at 28 °C, and a binary gradient of water/acetic acid (99.8:0.2) and methanol/acetonitrile (50:50) was used as mobile phases [flow rate of 0.8 mL/min; details are provided by Feng et al. (1)]. Five injections (in most cases, and 10 injections for phenols >150 μg) were conducted for each sample to collect ∼20–300 μg of each phenol (i.e., ∼10–150 μg of carbon) for ^{14}C measurement. After isolation, phenols were recovered from the aqueous mobile phase through extraction with ethyl acetate at pH 2 and eluted from a 5% deactivated SiO_2 column using ethyl acetate to remove potential column bleed. A small aliquot of purified phenols was derivatized with N,O-bis-(trimethylsilyl) trifluoroacetamide and pyridine to check compound purity by GC/MS, and was found to yield purities >99%. Purified phenols were transferred into precombusted quartz tubes in ethyl acetate and blown dry carefully under a gentle stream of N_2, with the addition of precombusted CuO afterward. The quartz tubes were evacuated on a vacuum line while immersed in an isopropanol/dry ice slush (−78 °C), flame-sealed, and combusted at 850 °C for 5 h. The resulting CO_2 was cryogenically purified and quantified by expansion into a calibrated volume. The procedural blanks were processed in the same manner.

Regional Temperature Data. Mean monthly temperatures (T_ms) recorded at climatic stations in the six watersheds (Fig. S3) from 1955 to 2004 were obtained from the Global Historical Climatology Network Monthly (GHCN-M, version 3; www.ncdc.noaa.gov/ghcnm/). In total, 102 climatic stations were identified within the great Russian Arctic river (GRAR) watersheds (Fig. S3). No climatic station within the Kalix drainage basin was found in the GHCN-M database. The five closest stations within 110 km from the watershed boundary were hence selected. Similarly, the GHCN-M database recorded only two climate stations within the Indigirka watershed. To increase the reliability of the Indigirka climatic data, we selected another three stations within 250 km from the watershed boundary.

We used annual summer cumulative temperature (ASCT) as a key temperature variable because summer temperatures are considered to have a major impact on permafrost thawing (2) and experience more variations than mean annual temperature during recent climate change (3). The value of the ASCT is given by the sum of mean T_ms for months with a T_m above 0 °C each year, and is thus related to the "thawing index" (4). The ASCT from 1985 to 2004 was calculated for each station separately and then averaged to represent the entire watershed.

1. Feng X, et al. (2013) ^{14}C and ^{13}C characteristics of higher plant biomarkers in Washington margin surface sediments. *Geochim Cosmochim Acta* 105:14–30.
2. Rinke A, et al. (2012) Arctic RCM simulations of temperature and precipitation derived indices relevant to future frozen ground conditions. *Global Planet Change* 80-81:136–148.
3. Hansen J, Sato M, Ruedy R (2012) Perception of climate change. *Proc Natl Acad Sci USA* 109(37):E2415–E2423.
4. Frauenfeld OW, Zhang T, McCreight JL (2007) Northern hemisphere freezing/thawing index variations over the twentieth century. *Int J Climatol* 27(1):47–63.

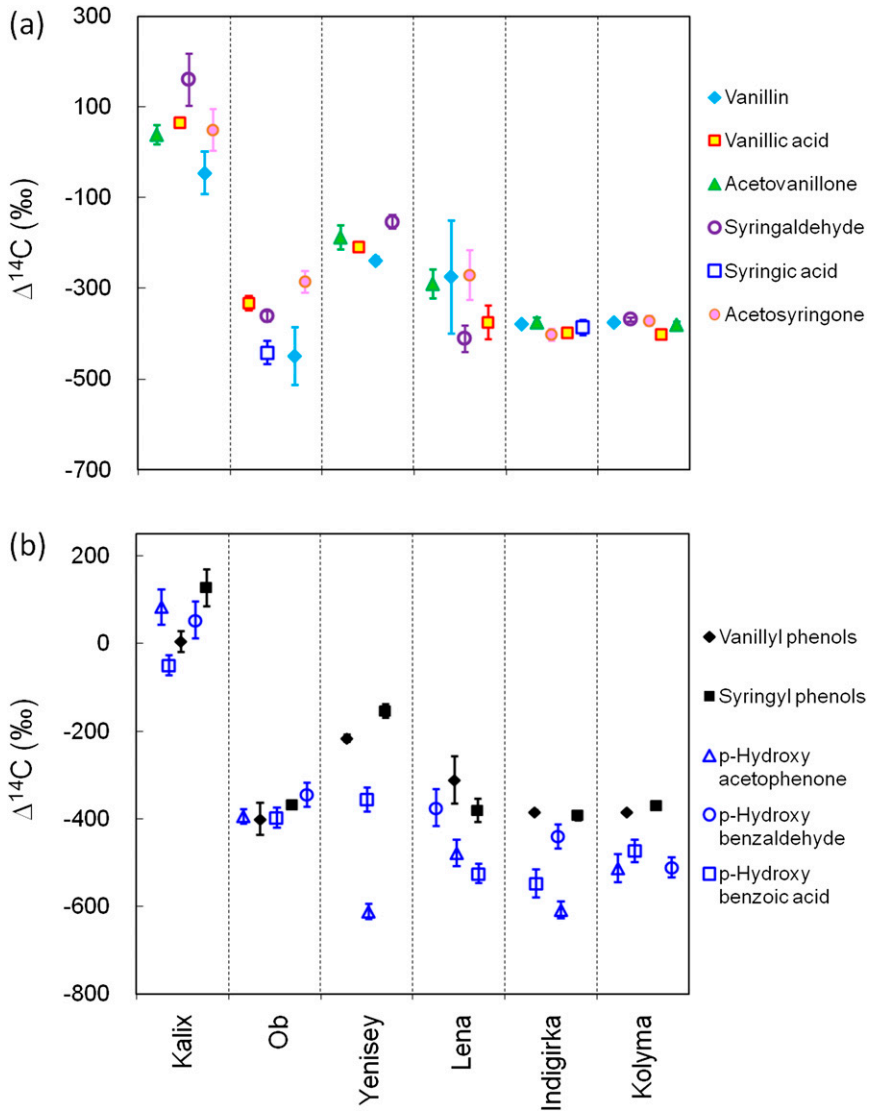

Fig. S1. $\Delta^{14}C$ values of individual lignin phenols (*A*) and individual hydroxy phenols (*B*) compared with the abundance-weighted average of vanillyl and syringyl phenols. All values are corrected for procedural blanks with the SEs of analytical measurement propagated. Note that there is no significant offset in the average $\Delta^{14}C$ values between vanillyl and syringyl phenols from the same estuarine sediment (*t* test, $P > 0.05$).

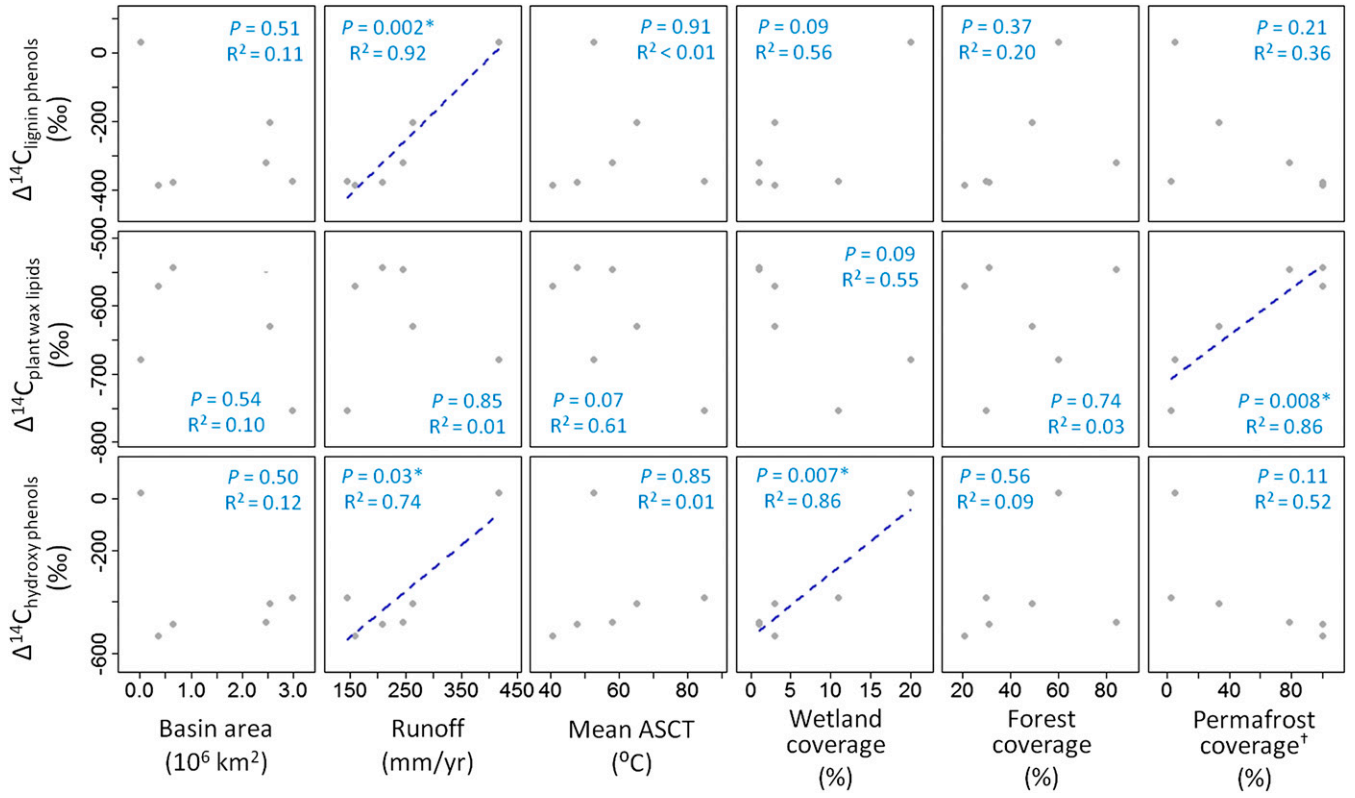

Fig. S2. Correlation between drainage basin characteristics and the $\Delta^{14}C$ values of terrestrial markers. Error bars represent the propagated SE of analytical measurement. *Linear correlation is considered to be significant at a level of $P < 0.05$, and the R^2 values are used to compare the explanatory power of the variables. †Continuous permafrost coverage. Note that runoff, continuous permafrost, and wetland coverage best explain the ^{14}C age of lignin phenols, plant wax lipids, and hydroxy phenols across the Eurasian Arctic, respectively. The ASCT is given for months with a mean temperature above 0 °C.

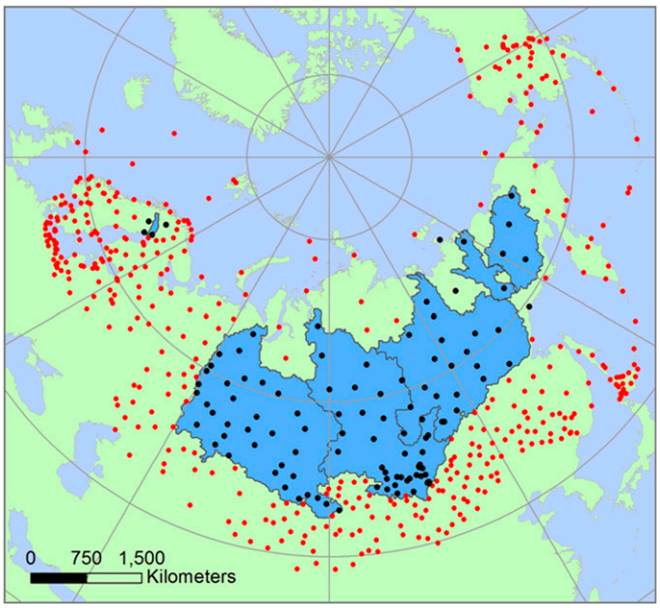

Fig. S3. Map of climatic stations recorded in the GHCN-M database for each drainage basin. The blue area represents the watersheds of great Russian Arctic rivers (GRARs) and the Kalix River; black and red points refer to the location of climatic stations included in the calculation of regional temperature data and for the interpolation method, respectively.

Table S1. Sample location, drainage basin characteristics, and bulk sediment properties of the great Russian Arctic rivers and Kalix River

Properties	Kalix	Ob	Yenisey	Lena	Indigirka	Kolyma
Latitude, longitude	65.44°N, 23.20°E	72.65°N, 73.44°E	72.61°N, 79.86°E	71.96°N, 129.54°E; 71.02°N, 132.60°E*	72.06°N, 150.46°E	70.00°N, 163.70°E
Geological and physiographic regions†	Scandinavian mountains	West Siberian lowlands	West Siberian lowlands	Central Siberian plateau	East Siberian highlands	East Siberian highlands
Mean ASCT (1985–2004), °C‡	53.7	87.4	65.4	57.9	40.7	47.9
Forest coverage, %§	60	30	49	84	21	31
Wetland coverage, %§	20	11	3	1	3	1
Permafrost coverage¶	5/15/80	2/24/74	33/55/12	79/20/1	100/0/0	100/0/0
Basin area, 10^6 km^2‖	0.024	2.54–2.99	2.44–2.59	2.40–2.49	0.34–0.36	0.65–0.66
Discharge, km^3/y**	10	427	673	588	54	136
Runoff, mm/y**	417	145	263	245	159	209
TOC/POC flux, t·km^{-2}·y^{-1}††	1.4/0.099	1.1/0.14	1.8/0.066	1.9/0.49	1.2/0.47	1.5/0.48
OC, %	4.5	0.9	1.9	0.5	1.5	1.7
OC/N‡‡	10.9 ± 0.3	10.0 ± 0.1	10.5 ± 0.1	12.3 ± 0.8	14.7 ± 0.2	15.9 ± 1.2
δ^{13}C-TOC, ‰	−27.1	−27.4	−26.5	−25.0	−26.6	−26.7
Δ^{14}C-TOC, ‰§§	−74 ± 37	−314 ± 3	−175 ± 3	−609 ± 3	−527 ± 3	−502 ± 2
^{14}C age of TOC, years B.P.§§	570 ± 250	3,000 ± 35	1,500 ± 30	7,500 ± 60	6,000 ± 50	5,600 ± 50

OC, organic carbon; POC, particulate organic carbon; TOC, total organic carbon.

*Combined surface sediments along a transect.

†According to the Arctic Monitoring and Assessment Programme (1).

‡ASCT was calculated as the sum of the mean T_m for months with a mean temperature above 0 °C within a year; temperature data were derived from the GHCN-M database.

§Data are from Ingri et al. (2) and "watersheds of the world" (http://archive.wri.org).

¶Given as % continuous; % (discontinuous + sporadic + isolated); % nonpermafrost (3, 4).

‖Data are from Ingri et al. (2), Gordeev et al. (5), Holmes et al. (6), and Rachold et al. (7).

**Data are from Ingri et al. (2), Holmes et al. (4), and Stein and Macdonald (8).

††Kalix data are from Ingri et al. (2); Great Russian Arctic River data are from Stein and Macdonald (8).

‡‡Mass ratio of OC to total nitrogen (9, 10).

§§Measured in 2006; values are normalized for the year of measurement.

1. AMAP (1998) *AMAP Assessment Report: Arctic Pollution Issues* (Arctic Monitoring and Assessment Programme, Oslo).
2. Ingri J, Widerlund A, Land M (2005) Geochemistry of major elements in a pristine boreal river system; hydrological compartments and flow paths. *Aquat Geochem* 11(1):57–88.
3. Gustafsson Ö, van Dongen BE, Vonk JE, Dudarev OV, Semiletov IP (2011) Widespread release of old carbon across the Siberian Arctic echoed by its large rivers. *Biogeosciences* 8: 1737–1743.
4. Holmes RM, et al. (2013) *Climatic Change and Global Warming of Inland Waters: Impacts and Mitigation for Ecosystems and Societies*, eds Goldman CR, Kumagai M, Robarts RD (Wiley, Chichester, UK), pp 3–26.
5. Gordeev VV, Martin JM, Sidorov IS, Sidorova MV (1996) A reassessment of the Eurasian river input of water, sediment, major elements, and nutrients to the Arctic Ocean. *Am J Sci* 296: 664–691.
6. Holmes RM, et al. (2002) A circumpolar perspective on fluvial sediment flux to the Arctic Ocean. *Global Biogeochem Cycles* 16:GB1098, 10.1029/2001GB001849.
7. Rachold V, et al. (2004) *The Organic Carbon Cycle in the Arctic Ocean*, eds Stein R, Macdonald RW (Springer, Berlin), pp 33–56.
8. Stein R, Macdonald RW (2004) *The Organic Carbon Cycle in the Arctic Ocean* (Springer, Berlin).
9. van Dongen BE, Semiletov I, Weijers JWH, Gustafsson Ö (2008) Contrasting lipid biomarker composition of terrestrial organic matter exported from across the Eurasian Arctic by the five great Russian Arctic rivers. *Global Biogeochem Cycles* 22:GB1011, 10.1029/2007GB002974.
10. Vonk JE, van Dongen BE, Gustafsson Ö (2008) Lipid biomarker investigation of the origin and diagenetic state of sub-arctic terrestrial organic matter presently exported into the northern Bothnian Bay. *Mar Chem* 112(1–2):1–10.
11. McClelland JW, Dery SJ, Peterson BJ, Holmes RM, Wood EF (2006) A pan-arctic evaluation of changes in river discharge during the latter half of the 20th century. *Geophys Res Lett* 33: L06715, 10.1029/2006GL025753.
12. Peterson BJ, et al. (2002) Increasing river discharge to the Arctic Ocean. *Science* 298(5601):2171–2173.

Table S2. Abundance of terrestrial OC markers in the estuarine surface sediments (milligrams per gram of OC) of the great Russian Arctic rivers and Kalix River

Compounds	Kalix	Ob	Yenisey	Lena	Indigirka	Kolyma
Lignin phenols*	14.35	13.36	11.15	11.41	21.37	22.78
Vanillin	4.06	3.11	2.94	3.64	4.58	5.17
Acetovanillone	2.04	1.80	1.76	2.30	3.68	3.38
Vanillic acid	2.34	2.35	2.38	2.78	3.62	3.69
Syringaldehyde	1.73	2.51	1.75	1.13	3.90	4.20
Acetosyringone	0.75	1.06	0.58	0.32	1.55	1.75
Syringic acid	1.42	1.45	0.87	0.67	2.16	2.60
p-Coumaric acid	1.60	0.56	0.52	0.40	0.78	0.93
Ferulic acid	0.41	0.52	0.34	0.18	1.11	1.05
Hydroxy phenols*	6.73	4.13	2.90	3.67	4.37	4.80
p-Hydroxybenzaldehyde	2.92	1.02	0.75	0.99	0.90	0.93
p-Hydroxyacetophenone	1.32	0.75	0.43	0.50	0.44	0.81
p-Hydroxybenzoic acid	2.49	2.36	1.72	2.18	3.03	3.06
Plant wax lipids†	0.44	0.91	0.62	0.44	1.22	1.17
$C_{27,29,31}$ *n*-alkanes†	0.16	0.76	0.48	0.28	0.91	0.65
$C_{24,26,28}$ *n*-alkanoic acids†	0.28	0.15	0.14	0.16	0.31	0.52

*Lignin and hydroxy phenols were measured on GC/MS as trimethylsilyl derivatives of CuO oxidation products.
†Plant wax lipids refer to the summary of $C_{27,29,31}$ *n*-alkanes and $C_{24,26,28}$ *n*-alkanoic acids measured previously (1, 2).

1. van Dongen BE, Semiletov I, Weijers JWH, Gustafsson Ö (2008) Contrasting lipid biomarker composition of terrestrial organic matter exported from across the Eurasian Arctic by the five great Russian Arctic rivers. *Global Biogeochem Cycles* 22:GB1011, 10.1029/2007GB002974.
2. Vonk JE, van Dongen BE, Gustafsson Ö (2008) Lipid biomarker investigation of the origin and diagenetic state of sub-arctic terrestrial organic matter presently exported into the northern Bothnian Bay. *Mar Chem* 112(1–2):1–10.

Table S3. Average $\Delta^{14}C$ values of lignin phenols in estuarine surface sediments of the great Russian Arctic rivers and Kalix River and contributions of modern surface OC to lignin estimated from the ^{14}C binary mixing model

Content	Kalix	Ob	Yenisey	Lena	Indigirka	Kolyma
Average $\Delta^{14}C$ of lignin phenols, ‰*	+33 ± 21	−375 ± 17	−203 ± 7	−320 ± 46	−385 ± 4	−379 ± 3
Percentage of modern surface OC in lignin, %						
When $\Delta^{14}C_S = +100‰$, $\Delta^{14}C_P = -655‰$†	91 ± 3	37 ± 2	60 ± 1	44 ± 6	36 ± 1	37 ± 1
When $\Delta^{14}C_S = +200‰$, $\Delta^{14}C_P = -655‰$†	80 ± 3	33 ± 2	53 ± 1	39 ± 6	32 ± 1	32 ± 1

*Abundance-weighted average values with errors propagated; original values are provided in Fig. S1.
†$\Delta^{14}C_S$ and $\Delta^{14}C_P$ refer to the $\Delta^{14}C$ value of surface and permafrost OC, respectively; the $\Delta^{14}C_P$ value is estimated from the regression relationship between lignin phenol $\Delta^{14}C$ values and runoff rate (Fig. 3*A*).

Table S4. Average $\Delta^{14}C$ values of terrestrial OC pools (represented by different groups of markers) and contributions of surface vs. deep permafrost OC to terrestrial biospheric OC in surface sediments of the great Russian Arctic rivers and Kalix River in 2004 and 1985

Content	Kalix	Ob	Yenisey	Lena	Indigirka	Kolyma
Average $\Delta^{14}C$ value of terrestrial biospheric OC (represented by hydroxy phenols)*	+22 ± 22	−383 ± 15	−404 ± 23	−477 ± 18	−529 ± 23	−486 ± 18
Current budget (2004)						
Average $\Delta^{14}C$ value of terrestrial OC pools, ‰						
Surface-dominated OC (represented by lignin phenols)*	+33 ± 21	−375 ± 17	−203 ± 7	−320 ± 46	−385 ± 4	−379 ± 3
Deep permafrost-dominated OC (represented by plant wax lipids)†	−679 ± 43	−753 ± 6	−630 ± 7	−546 ± 6	−571 ± 10	−543 ± 9
Contribution of OC pools, %‡						
Surface OC	98 ± 2	98 ± 2	53 ± 5	31 ± 8	23 ± 13	35 ± 11
Deep permafrost OC	2 ± 2	2 ± 2	47 ± 5	69 ± 8	77 ± 13	65 ± 11
Budget of the past (1985)						
Average $\Delta^{14}C$ value of terrestrial OC pools, ‰						
Surface-dominated OC (represented by lignin phenols)§	+9 ± 21	−399 ± 17	−227 ± 7	−344 ± 46	−404 ± 4	−403 ± 3
Deep-permafrost-dominated OC (represented by plant wax lipids)§	−679 ± 43	−753 ± 6	−630 ± 7	−546 ± 6	−571 ± 10	−543 ± 9
Contribution of OC pools (%)‡						
Surface OC	nc¶	nc¶	56 ± 5	34 ± 8	25 ± 13	41 ± 11
Deep permafrost OC	nc¶	nc¶	44 ± 5	66 ± 8	75 ± 13	59 ± 11

*Abundance-weighted average values with errors propagated, original values are provided in Fig. S1.

†Original values of long-chain *n*-alkanes and *n*-alkanoic acids are taken from Gustafsson et al. (1).

‡Estimated from the ^{14}C binary mixing model (Eq. **1**), where the $\Delta^{14}C$ value of terrestrial biospheric OC is represented by that of hydroxyl phenols (derived from both surface OC and deep permafrost), whereas surface and deep permafrost end-member values ($\Delta^{14}C_S$ and $\Delta^{14}C_P$) equal those of lignin phenols and plant wax lipids in each basin, respectively. Hence, $f_{surface} = (\Delta^{14}C_{hydroxy\ phenols} - \Delta^{14}C_{plant\ wax\ lipids})/(\Delta^{14}C_{lignin\ phenols} - \Delta^{14}C_{plant\ wax\ lipids})$.

§Based on the linear relationship between lignin phenol $\Delta^{14}C$ values and runoff ($\Delta^{14}C = 1.6018 \times$ runoff $- 655$; Fig. 3*A*) and the runoff increasing rate of ∼0.60 (Indigirka) to 0.74 mm/y [the other great Russian Arctic rivers (GRARs)] from 1964 to 2000 in Eurasian Arctic rivers (2, 3). Lignin phenol $\Delta^{14}C$ values are estimated to be lower by 19‰ [0.60 mm/y × 20 y × 1.6018‰/(mm/y) for Indigirka] to 24‰ [0.74 mm/y × 20 y × 1.6018‰/(mm/y) for the other big GRARs] in 1985 compared with those measured in 2004 (not considering the dilution of bomb ^{14}C in the atmosphere). The $\Delta^{14}C$ values of plant wax lipid and hydroxy phenols are assumed to remain the same as in 2004.

¶Past OC contribution in the Kalix and Ob is not calculated (nc) because the estimated $\Delta^{14}C$ values of surface OC (lignin phenols) are lower than those of terrestrial biospheric OC (hydroxy phenols).

1. Gustafsson Ö, van Dongen BE, Vonk JE, Dudarev OV, Semiletov IP (2011) Widespread release of old carbon across the Siberian Arctic echoed by its large rivers. *Biogeosciences* 8: 1737–1743.
2. McClelland JW, Dery SJ, Peterson BJ, Holmes RM, Wood EF (2006) A pan-arctic evaluation of changes in river discharge during the latter half of the 20th century. *Geophys Res Lett* 33: L06715, 10.1029/2006GL025753.
3. Peterson BJ, et al. (2002) Increasing river discharge to the Arctic Ocean. *Science* 298(5601):2171–2173.